AMERICAN SOCIETY FOR MICROBIOLOGY | Applied and Environmental Microbiology®

FOOD MICROBIOLOGY

Mycotoxin Biosynthesis and Central Metabolism Are Two Interlinked Pathways in *Fusarium graminearum*, as Demonstrated by the Extensive Metabolic Changes Induced by Caffeic Acid Exposure

Vessela Atanasova-Penichon,[a] Laurie Legoahec,[a] Stéphane Bernillon,[b,c] Catherine Deborde,[b,c] Mickaël Maucourt,[b,c] Marie-Noëlle Verdal-Bonnin,[a] Laetitia Pinson-Gadais,[a] Nadia Ponts,[a] Annick Moing,[b,c] Florence Richard-Forget[a]

[a]UR1264 MycSA, INRA, Centre INRA de Nouvelle Aquitaine—Bordeaux, Villenave d'Ornon, France

[b]UMR1332 Biologie du Fruit et Pathologie, INRA, Université de Bordeaux, Centre INRA de Nouvelle Aquitaine—Bordeaux, Villenave d'Ornon, France

[c]Metabolome Facility of Bordeaux Functional Genomics Center, MetaboHUB, IBVM, Centre INRA de Nouvelle Aquitaine—Bordeaux, Villenave d'Ornon, France

ABSTRACT *Fusarium graminearum* is a major plant pathogen that causes devastating diseases of cereals and produces type B trichothecene (TCTB) mycotoxins in infected grains. A comprehensive understanding of the molecular and biochemical mechanisms underlying the regulation of TCTB biosynthesis is required for improving strategies to control the TCTB contamination of crops and ensuring that these strategies do not favor the production of other toxic metabolites by *F. graminearum*. Elucidation of the association of TCTB biosynthesis with other central and specialized processes was the focus of this study. Combined ^{1}H nuclear magnetic resonance (^{1}H NMR) and liquid chromatography-quadrupole time of flight-mass spectrometry (LC-QTOF-MS) analyses were used to compare the exo- and endometabolomes of *F. graminearum* grown under toxin-inducing and -repressing caffeic acid conditions. Ninety-five metabolites were putatively or unambiguously identified, including 26 primary and 69 specialized metabolites. Our data demonstrated that the inhibition of TCTB production induced by caffeic acid exposure was associated with significant changes in the secondary and primary metabolism of *F. graminearum*, although the fungal growth was not affected. The main metabolic changes were an increase in the accumulation of several polyketides, including toxic ones, alterations in the tricarboxylic organic acid cycle, and modifications in the metabolism of several amino acids and sugars. While these findings provide insights into the mechanisms that govern the inhibition of TCTB production by caffeic acid, they also demonstrate the interdependence between the biosynthetic pathway of TCTB and several primary and specialized metabolic pathways. These results provide further evidence of the multifaceted role of TCTB in the life cycle of *F. graminearum*.

IMPORTANCE *Fusarium graminearum* is a major plant pathogen that causes devastating diseases of cereal crops and produces type B trichothecene (TCTB) mycotoxins in infected grains. The best way to restrict consumer exposure to TCTB is to limit their production before harvest, which requires increasing the knowledge on the mechanisms that regulate their biosynthesis. Using a metabolomics approach, we investigated the interconnection between the TCTB production pathway and several fungal metabolic pathways. We demonstrated that alteration in the TCTB biosynthetic pathway can have a significant impact on other metabolic pathways, including the biosynthesis of toxic polyketides, and vice versa. These findings open new avenues for identifying fungal targets for the design of molecules with antimycotoxin properties and therefore improving sustainable strategies to fight against dis-

Received 7 August 2017 **Accepted** 30 January 2018

Accepted manuscript posted online 2 February 2018

Citation Atanasova-Penichon V, Legoahec L, Bernillon S, Deborde C, Maucourt M, Verdal-Bonnin M-N, Pinson-Gadais L, Ponts N, Moing A, Richard-Forget F. 2018. Mycotoxin biosynthesis and central metabolism are two interlinked pathways in *Fusarium graminearum*, as demonstrated by the extensive metabolic changes induced by caffeic acid exposure. Appl Environ Microbiol 84:e01705-17. https://doi.org/10.1128/AEM.01705-17.

Editor Emma R. Master, University of Toronto

Address correspondence to Vessela Atanasova-Penichon, vessela.atanasova@inra.fr.

eases caused by *F. graminearum*. Our data further demonstrate that analyses should consider all fungal toxic metabolites rather than the targeted family of mycotoxins when assessing the efficacy of control strategies.

KEYWORDS *Fusarium*, caffeic acid, metabolome, mycotoxins

Of several hundred different mold species, fungi of the *Fusarium* genus are the most important in the more temperate and colder parts of the world (e.g., central and northern Europe and northern America) with respect to crop spoilage and mycotoxin contamination within agricultural production. Thus, in the published "top 10" plant fungal pathogen list established according to scientific and economic criteria (1), *Fusarium graminearum* and *Fusarium oxysporum* rank at the fourth and fifth places, respectively. *F. graminearum*, which is responsible for *Fusarium* head blight (FHB) in wheat and barley and ear rot in maize, is also the major producer of mycotoxins belonging to the type B trichothecene (TCTB) group (2). This group includes deoxynivalenol (DON) and its derivatives 3-acetyldeoxynivalenol (3-ADON) and 15-acetyldeoxynivalenol (15-ADON), as well as nivalenol (NIV) and its 4-acetyl derivative fusarenon X (FX). DON has been recognized as a major food- and feed-contaminating toxin, and since 2005, regulatory values have been established for DON in European cereals and cereal products (EC no. 856/2005). These values were revised in July 2007 (EC no. 1126/2007). Being particularly stable, TCTBs resist agri-food processing and remain in finished cereal products. The guarantee of the safety of cereal products therefore depends on preventive actions that are taken during the cultivation of cereals. Currently, there is no existing cultivation strategy that is sufficiently effective in limiting contamination with TCTB to certify compliance with official limits. A comprehensive understanding of the molecular and biochemical mechanisms underlying the regulation of TCTB biosynthesis is required for improving or developing novel strategies to efficiently manage the risks posed by *F. graminearum*. The TCTB biosynthetic pathway is fairly well elucidated (3, 4). Trichodiene, the first committed intermediate in the TCTB biosynthetic pathway, results from the cyclization of farnesyl pyrophosphate. The sequence of chemical reactions (oxygenations, isomerizations, cyclizations, and esterifications) together with the structures of the chemical intermediates have been characterized, from trichodiene to the end products, including DON and ADON (5). Nearly all the genes implicated in the TCTB biosynthetic pathway, commonly named *TRI* genes, have been identified (6). Most of them are localized in one genomic locus, which is referred as the "FgTRI5 cluster." Among the 15 characterized *TRI* genes, two pathway-specific transcription factors, *TRI6* and *TRI10*, have been identified. However, it is now clearly established that the major control of TCTB production is exerted by various transcriptional regulators known to regulate basal metabolic functions in fungi (4, 7, 8). Regulatory circuits that govern the fungal responses to changes in environmental factors, such as responses to pH via the *Pac* transcription factor (9, 10) or to light via the velvet complex (11) or the response to oxidative stress via the *FgAp1* factor (12), were shown to control TCTB production. In spite of this enhanced knowledge of the regulation of the TCTB biosynthetic pathway, the interconnections between the general regulatory circuits able to affect TCTB production remain to be detailed. Deciphering this interconnection first requires the elucidation of how TCTB biosynthesis integrates with central and secondary or specialized metabolic pathways. The use of metabolomics could be one promising way to tackle this challenge. Metabolomics aims at analyzing the entire complement of metabolites produced by a biological system. As the downstream product of gene transcription and proteome expression, the metabolome is tightly coupled to the phenotype of the biological system studied and is highly sensitive to genetic and environmental stimuli (13). Relatively few metabolomics studies have been reported for filamentous fungi, and when they are available, these studies are frequently incomplete since they focus mainly on central metabolism, carbon flux, and energy turnover. Thus, the central metabolome of *F. oxysporum* was characterized under different cultivation conditions (14), the central

metabolome of *F. graminearum* strains was compared with those of *Fusarium culmorum*, *Fusarium pseudograminearum*, and *Fusarium venetatum* strains (15), and the impact of iron on the central metabolome of *Cryptococcus neoformans* was investigated (16). In rare reports, the specific production of one secondary metabolite was included in addition to central metabolome profiling. This was the case for the production of penicillin in *Penicillium chrysogenum* (17), of fumonisin in *Fusarium verticillioides* (18), and of beauvericin in *Cordyceps bassania* (19). A first attempt to link TCTB production and basal metabolism in *F. graminearum* was developed by Chen et al. (20). Using a *tri5* deletion strain, i.e., a strain that has lost its ability to produce DON, these authors showed that affecting TCTB production induced significant changes in both carbon and nitrogen metabolism. This study was, however, restricted to the *F. graminearum* endometabolome and did not address the link between TCTB biosynthesis and other secondary metabolic pathways. Indeed, along with TCTB, *F. graminearum* can produce a wide array of secondary metabolites, including polyketides and nonribosomal peptides. A whole-genome analysis (21) has revealed the presence of genes encoding 15 polyketide synthases (PKS) and 19 nonribosomal peptide synthases (NRPS) in *F. graminearum*. According to Hansen et al. (22), the products of 7 of the 15 polyketide synthases and 16 of the 19 nonribosomal peptide synthetases have not yet been identified. Among the currently known polyketides, the bioactive metabolites zearalenone, fusarins, and more recently the fusarielins (23) are the most frequently reported, together with the aurofusarin and rubrofusarin pigments, the fusarubins, fusaristatins, and orcinol (22). Malonichrome, ferricrocin, and fusarinine are the three nonribosomal peptides for which production has been associated with the identified nonribosomal peptide synthase-encoding genes in *F. graminearum* (21).

The main objective of this study was to elucidate the relationship between TCTB biosynthesis and other central and secondary metabolic processes. To achieve this objective, we have compared the intracellular and extracellular metabolite profiles of *F. graminearum* growing under toxin-inducing or -repressing conditions. Repressing conditions were achieved using caffeic acid, the toxin-inhibiting effects of which have been demonstrated in recent publications (24). By applying this strategy, our study will provide additional information on the yet not fully understood mechanism that governs the inhibition of TCTB production by caffeic acid and will reveal whether the use of caffeic acid to control the contamination with TCTB does not favor the biosynthesis of another group of toxic metabolites produced by *F. graminearum*.

RESULTS

Inhibition of TCTB production by caffeic acid. The effect of 0.5 mM caffeic acid on fungal growth and TCTB production by *F. graminearum* CBS 185.32 was evaluated on days 3, 5, 7, and 14 after inoculation. Fungal growth was not significantly affected by the supplementation with 0.5 mM caffeic acid (Fig. 1A). Biomass was monitored: accumulation began 24 h after inoculation and increased sharply until the third to fifth days of culture (exponential phase of growth). Then, the kinetics of biomass accumulation slowed down, and the cells reached the stationary phase of growth after 5 days of culture (Fig. 1A). DON and 15-ADON were first detected in supernatants after 3 days of culture (Fig. 1B). TCTB accumulation was nearly linear between days 3 and 14, with toxin yields reaching 17.2 mg/g in control cultures. After 14 days of growth in the presence of caffeic acid, TCTB levels were reduced by 52%. In the presence of caffeic acid, TCTB levels were not detectable at day 3 and then were reduced by 88% at day 5, 74% at day 7, and 52% after 14 days of growth relative to levels in control cultures (Fig. 1B). These results are consistent with those obtained by Gauthier et al. (24), who used the same *F. graminearum* CBS 185.32 strain in liquid medium supplemented or not with caffeic acid. When assayed in mycelia, TCTBs were first quantified in 5-day-old mycelia (Fig. 1A). In control samples, their accumulation drastically increased between days 5 and 7 and then remained stable between days 7 and 14 to reach a value of 0.21 mg/g in 14-day-old mycelia. In caffeic acid-supplemented samples, toxin accumulation gradually increased between days 3 and 7 and then sharply increased between days 7

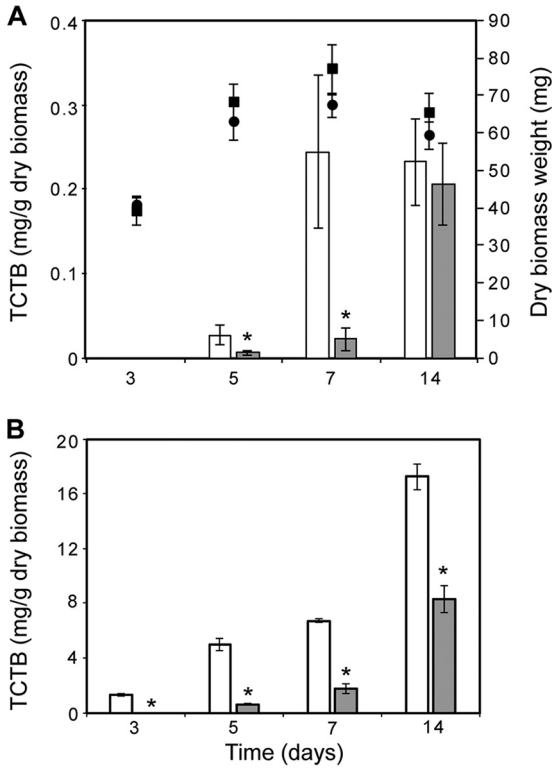

FIG 1 Kinetics of biomass and TCTB accumulation by *F. graminearum* in control and caffeic acid-treated cultures. Kinetics of biomass (circles and squares) and TCTB accumulation (bars) in mycelia (A) and in supernatants (B) of *F. graminearum* CBS 185.32 grown under control conditions (white bars and circles) and in 0.5 mM caffeic acid-supplemented cultures (gray bars and squares) are shown. *, significant difference compared with control treatment (Student's *t* test, $P < 0.05$). Data are means ± standard deviations for four biological replicates.

and 14 to reach the same levels as in the control (not supplemented) samples in 14-day-old mycelia (Fig. 1A). Unlike those in supernatants, TCTB levels in mycelia were identical in control and caffeic acid-supplemented samples after 14 days of incubation. At days 5 and 7, TCTB accumulation was significantly lower in caffeic acid-supplemented samples than in control ones, and these diminutions were 78% and 91%, respectively.

Metabolomics characterization of *F. graminearum* at different developmental stages. The ^{1}H nuclear magnetic resonance (^{1}H NMR) and liquid chromatography-quadrupole time of flight mass spectrometry (LC-QTOF-MS) spectra of fungal mycelium extracts (endometabolome) and of culture supernatants (exometabolome), in the absence of exogenous caffeic acid, obtained in the exponential (3- and 5-day-old cultures) and stationary (7- and 14-day-old cultures) phases of growth allowed us to detect 95 metabolites: 18 in supernatants, 42 in mycelia, and 35 common to both supernatants and mycelia (see Table S1 in the supplemental material).

Biomolecules were unambiguously or putatively identified according to their proton chemical shifts compared to database values and spectra of authentic standards (^{1}H NMR) (see Table S2 in the supplemental material) or based on *m/z* signal, accurate mass measurement, and literature data (25–27) on fungal metabolites (LC-QTOF-MS) (see Table S3 in the supplemental material) (28). The identification status of each metabolite is indicated according to the Metabolomics Standards Initiative (Tables S2 and S3). Primary metabolites included 13 amino acids and 2 derivatives (choline and γ-aminobutyrate [GABA]), 4 organic acids of the tricarboxylic acid (TCA) cycle, 3 sugars, and 4 cofactors (nucleosides and nucleotides). Our data sets contain 69 secondary metabolites classified into three major groups: sesquiterpenes, polyketides, and "others." Along with DON and 15-ADON, which are the major TCTBs known to be produced

by the strain used in this study, 53 sesquiterpenes were detected, including 13 intermediates of the TCTB biosynthetic pathways and their isomers (Table S1). Ten compounds were identified as polyketides, which are frequently considered the most abundant fungal secondary metabolites (26) and whose biosynthesis is catalyzed by type I polyketide synthases. This group comprises four naphthoquinone pigments (aurofusarin and its isomer, rubrofusarin, and novarubin), four zearalenone derivatives (5-formyzearalenone and its three isomers), one bibenzoquinone (oosporein), and the cyclic lipopeptide fusaristatin A, for which a biosynthetic gene cluster in the *F. graminearum* genome has recently been described (29). The third group of secondary metabolites was named "others" and includes butenolide, dimerumate, phenylacetate, fusarinine like_1, and fusarinine like_2. The two latter metabolites were characterized by identical masses (Table S3), but while fusarinine like_1 was detected in mycelia at a retention time of 3.35 min, fusarinine like_2 was detected in supernatants at a retention time close to 7.89 min. Such differences in retention times raised doubts about the identity of these compounds and led us to include "like" in their name.

Primary metabolites were detected exclusively in mycelia with the exceptions of Asn, arabitol, and trehalose, which were also retrieved from supernatants. Thirty-five secondary metabolites, most of the sesquiterpenes and "others," were found in both mycelia and supernatants. Sesquiterpenes such as trichodiene and the majority of 15-decalonectrin or 8-hydroxytrichodermin (8-H-trichodermin) isomers, 2-H-trichodiene isomers, and polyketides such as oosporein, aurofusarin, rubrofusarin, and fusaristatin A were isolated only from mycelia.

The metabolites gathered in Table S1 were integrated into a putative and simplified metabolic map that we generated using literature data (Fig. 2). This metabolic map provides a framework that enables visualization of the connections that can occur between the metabolic pathways and can guide the biological interpretations associated with modifications in metabolite profiles. To dissect the temporal changes in abundance of the 95 metabolites previously reported (Table S1), we used K-means clustering for the control condition of culture supernatants and mycelia, separately. For mycelium extracts, K-means clustering of 77 compounds resulted in 5 clusters of analytes corresponding to four clearly different accumulation patterns (Fig. 3). The first cluster comprises mainly amino acids/amino acid derivatives, nucleosides/nucleotides, and butenolide, the intracellular levels of which exhibited a progressive decrease throughout the 14 days of culture (Fig. 3A). TCA cycle intermediates such as malate, fumarate, and succinate, the rest of the amino acids (Tyr, Ile, and Phe), and nucleosides/nucleotides (adenosine-like), as well as sugars, were the major metabolites included in cluster 2 (Fig. 3B). Their intracellular concentrations were shown to increase until 5 days of culture (exponential growth phase) and then sharply decrease. Secondary metabolites were divided into three clusters and two main profiles. Temporal changes of metabolites in clusters 3 and 4 (most of the sesquiterpenes, including DON, 15-ADON, and polyketides) were similar until 7 days of culture; i.e., there was a slight increase between days 3 and 5 (exponential phase of growth) and a marked increase between days 5 and 7 (beginning of stationary phase) (Fig. 3C and D). After 7 days of culture, intracellular levels of metabolites of cluster 3 (Fig. 3C) significantly increased, while levels of metabolites of cluster 4 (Fig. 3D) significantly declined. The changes of metabolite concentration for cluster 5 (several sesquiterpenes, citrate, fusaristatin A, novarubin, aurofusarin_1, and dimerumate) were similar to those for cluster 4, with the exception of a continuous increase in metabolite concentrations during the fungal exponential phase (Fig. 3E).

For culture supernatants, the 53 compounds were clustered into four groups (Fig. 4) and revealed three main patterns. Extracellular levels of metabolites included in the first two clusters (Fig. 4A and B) shared a quite similar profile, i.e., a continuous and gradual accumulation throughout the 14 days of culture. 15-ADON was included in the first cluster, in addition to several sesquiterpenes and novarubin. Cluster 2 comprises exclusively compounds of the sesquiterpene group, including DON. Metabolites classified in cluster 3 (Fig. 3C) exhibited a linear increase in their abundance during the 7

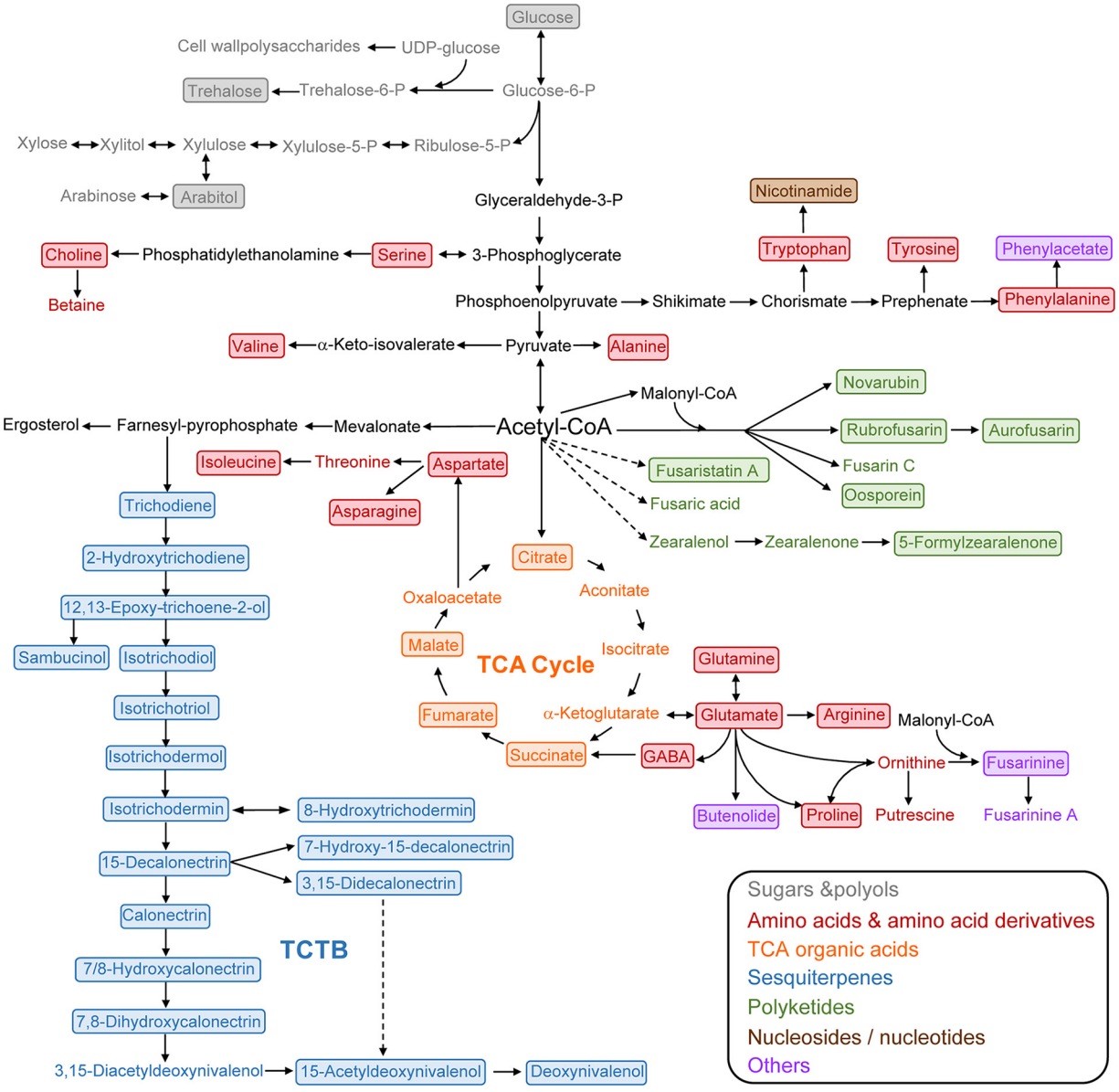

FIG 2 Overview of metabolic pathways, indicating the relationship between the production of TCTB by *F. graminearum* and other primary and secondary metabolic pathways. Many steps and compounds are omitted for simplification. Metabolites detected in *F. graminearum* supernatants and/or mycelia are boxed.

first days of culture (i.e., during the exponential growth phase and the beginning of the stationary phase) followed by a plateau phase until the end of the cultures. Four sesquiterpenes (7/8-H-calonectrin, 7,8-di-H-calonectrin_1, and isotrichodermol_1 and _5) and two sugars or polyols (trehalose and arabitol) belong to cluster 3, in addition to fusarinine-like_2, phenylacetate, dimerumate, and 5-formylzearalenone_2. 5-Formylzearalenone isomers, trichodiol or isotrichodiol_2, isotrichodermol_4, Asp, and butenolide are the core representatives of cluster 4 (Fig. 4D). Their pattern showed an increase or stability during the first 7 days of culture (i.e., during the exponential growth phase and beginning of the stationary phase) followed by a decrease until the end of the cultures.

Alterations in the endo- and exometabolomes of *F. graminearum* when exposed to caffeic acid. In order to evaluate whether endo and exo-metabolome profiles discriminate between the control and the caffeic acid-treated conditions during the

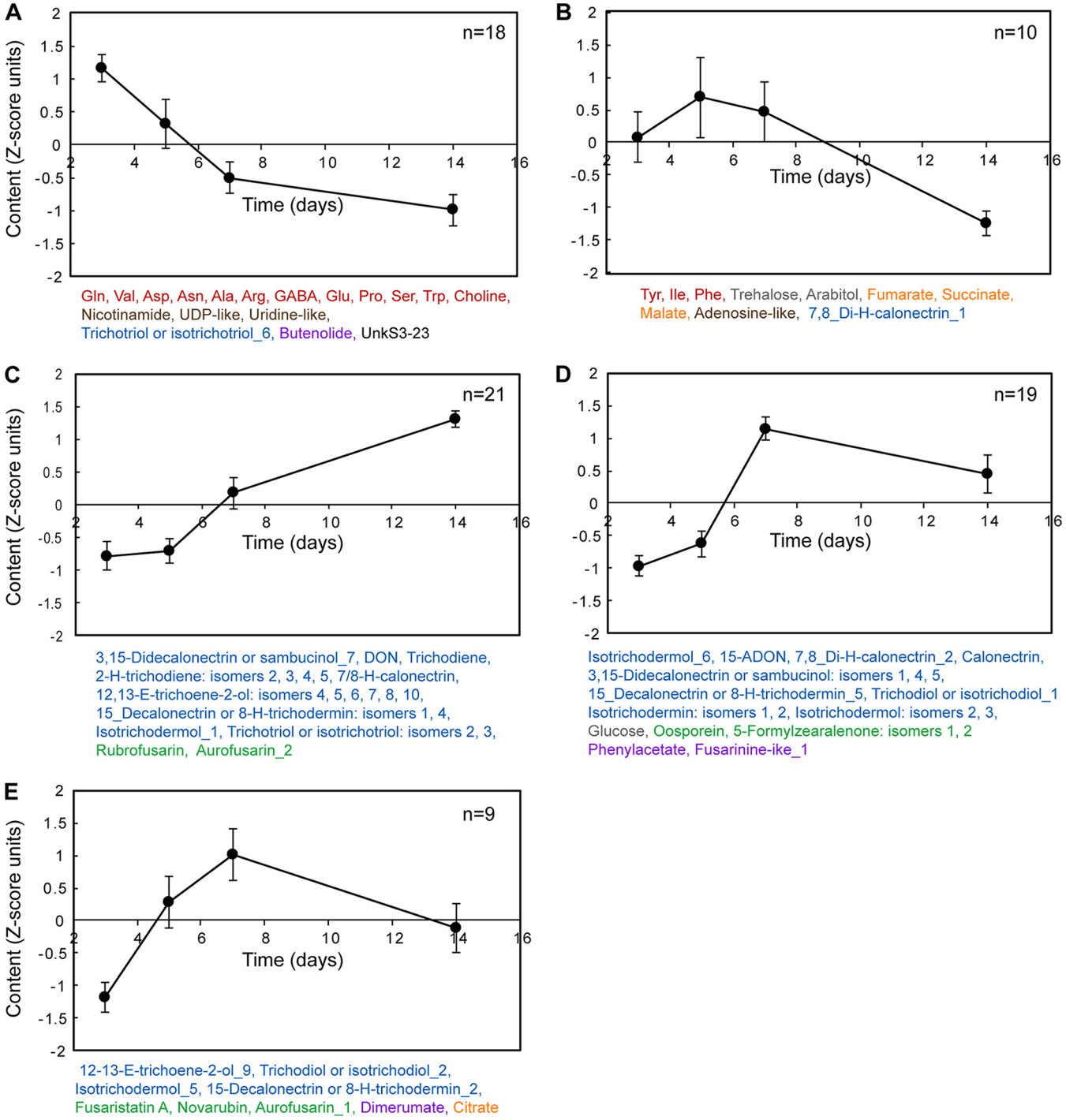

FIG 3 Accumulation patterns of 77 metabolites in *F. graminearum* control mycelia. Five patterns (A to E) were inferred through K-means clustering. The circles represent the mean of all compounds in each cluster. Vertical bars represent the standard deviation. The names of compounds in each cluster are reported: gray, sugars and polyols; red, amino acids and amino acid derivatives; orange, TCA organic acids; blue, sesquiterpenes; green, polyketides; brown, nucleosides and nucleotides; purple, others; and black, unknown compounds. H, hydroxy; E, epoxy.

time of culture, principal-component analyses (PCA) were performed for mycelia (Fig. 5) and supernatants (Fig. 6) separately.

The PCA scores plots (Fig. 5A and 6A) show the distribution of treated/control samples in the plane defined by the first two components, which explained 66% and 84% of the total variance for mycelia and supernatants, respectively. Samples harvested during the exponential phase of fungal growth (3 and 5 days of culture) were separated

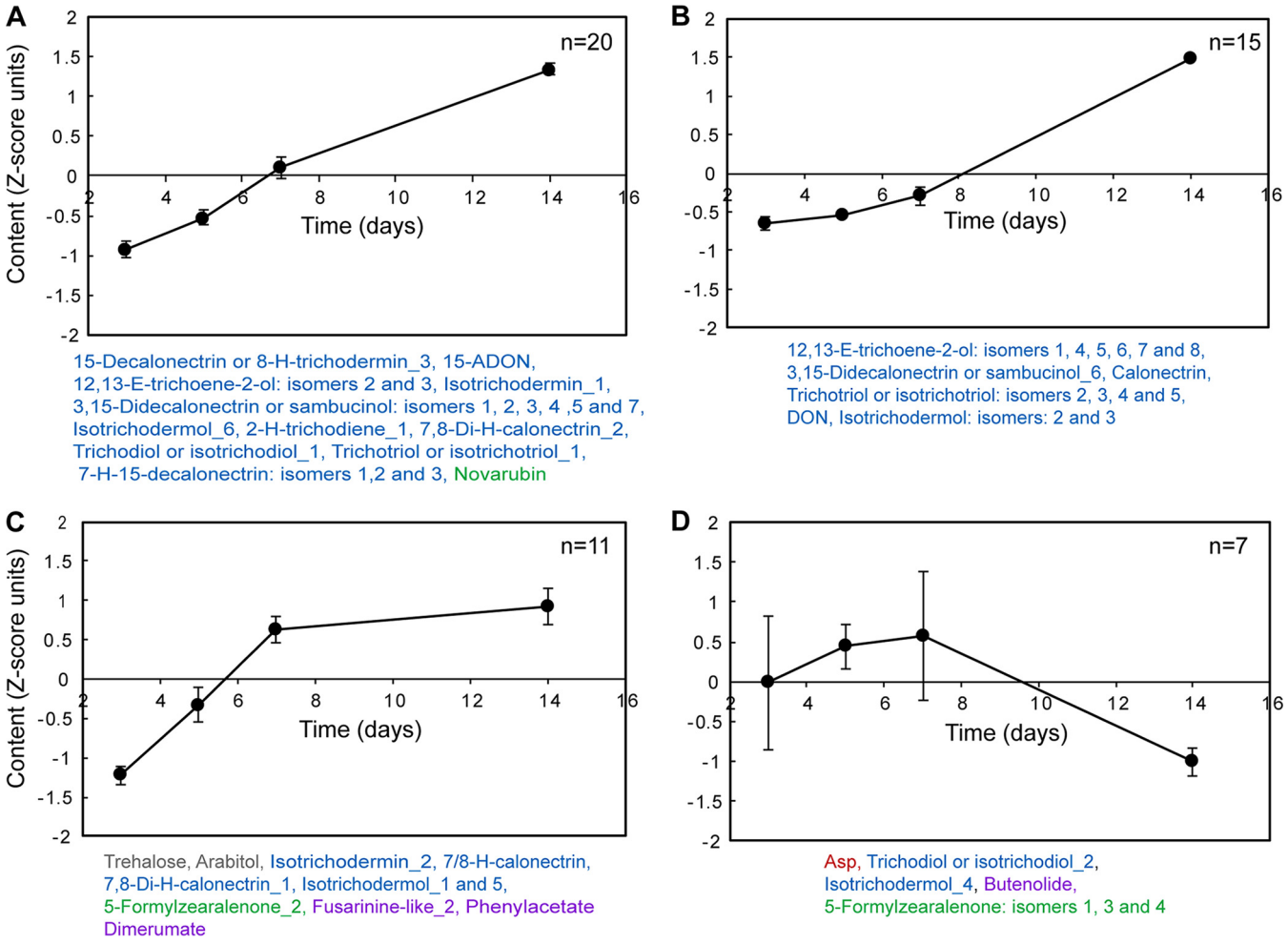

FIG 4 Accumulation patterns of 53 metabolites in *F. graminearum* control supernatants. Four patterns (A to D) were inferred through K-means clustering. The circles represent the mean of all compounds in each cluster. Vertical bars represent the standard deviation. The names of compounds in each cluster are reported: gray, sugars and polyols; red, amino acids and amino acid derivatives; blue, sesquiterpenes; green, polyketides; and purple, others. H, hydroxy; E, epoxy.

from samples collected in the stationary phase (7 and 15 days of culture) as a function of culture duration along the first axis, which can thus be interpreted as a "time" axis with time increasing from left to right. This axis contributed 51% and 73% to the total variance for mycelia and supernatants, respectively. Between the control and caffeic acid-treated samples, PCA analyses showed that at late time points (day 7 for mycelia and day 14 for supernatants), metabolomic profiles were significantly different, while the metabolomic profiles at early time points (3 and 5 days) tended to cluster together for both the control and treated samples. For these late time points, caffeic acid-supplemented and control samples were separated along the second axis, which could thus be interpreted as a "caffeic acid treatment" axis. This second axis explained 15% (mycelia) or 11% (supernatants) of the total variability of the data.

The comparison of the PCA score plots (Fig. 5A and 6A) and loading plots (Fig. 5B and 6B) show which metabolites or group of metabolites may contribute to the separations observed in the scores plots. As evidenced in Fig. 5B, compounds produced by secondary metabolism, such as sesquiterpenes (including DON and 15-ADON), polyketides, and phenylacetate, positively contributed to the loadings of PC1, while metabolites from primary metabolism, such as amino acids/amino acid derivatives, sugars/polyols (trehalose and arabitol), and nucleosides/nucleotides, contributed negatively. In regard to PC2, the metabolites contributing the most to the discrimination

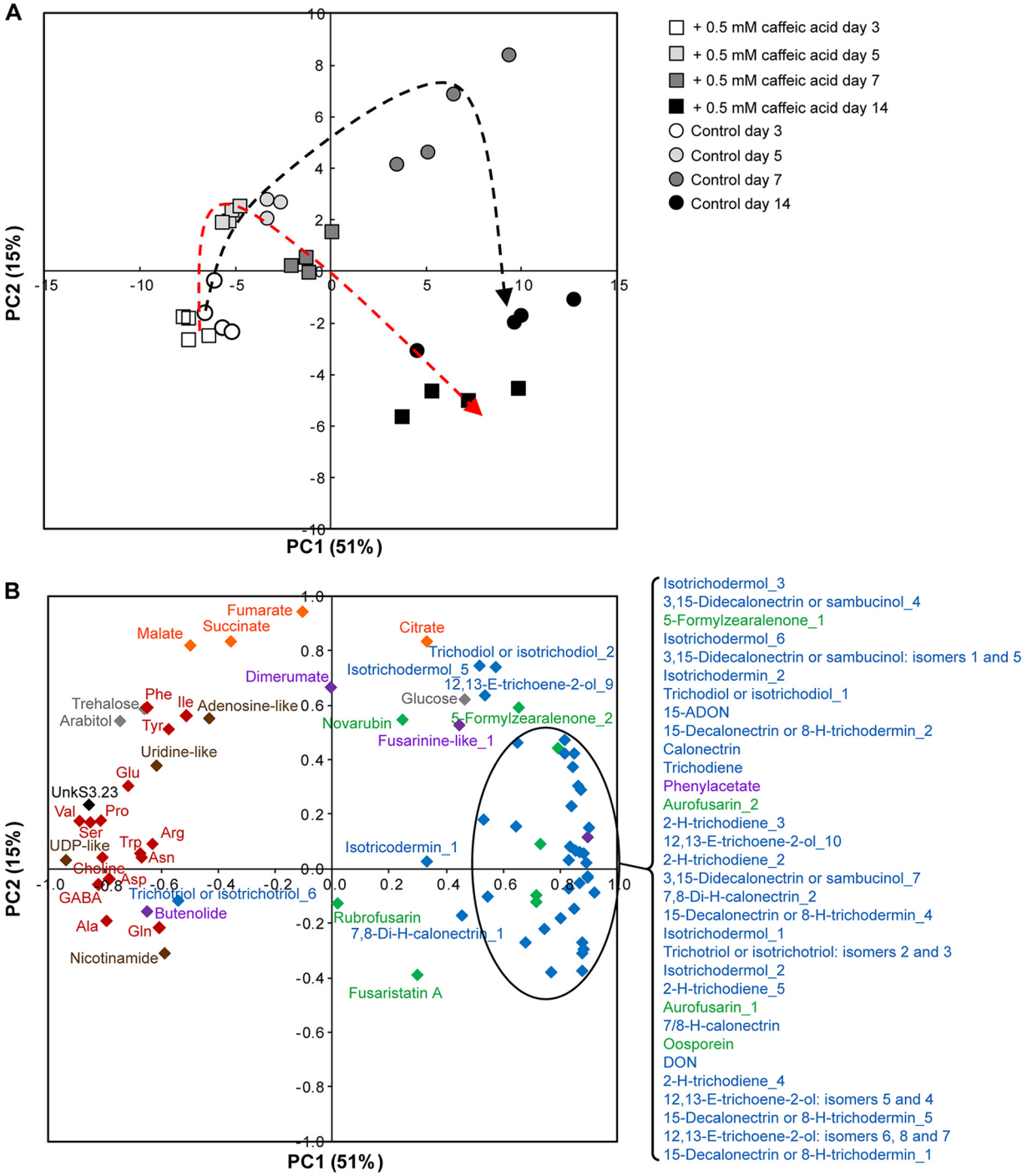

FIG 5 Caffeic acid modifies the endometabolome of *F. graminearum*. Principal-component analysis score (A) and loading (B) plots for 77 metabolites in *F. graminearum* mycelia supplemented (squares) or not (circles) with 0.5 mM caffeic acid are shown. White, day 3; light gray, day 5; dark gray, day 7; black, day 14. The names of the metabolites are reported: gray, sugars and polyols; red, amino acids and amino acid derivatives; orange, TCA organic acids; blue, sesquiterpenes; green, polyketides; brown, nucleosides and nucleotides; purple, others; and black, unknown compounds. H, hydroxy; E, epoxy.

were TCA organic acids. Besides TCA organic acids although to a lesser extent, glucose and several secondary metabolites, including novarubin, 5-formylzearalenone isomers 1 and 2, fusarinine-like_1, and various first intermediates of the TCT biosynthesis pathway positively contributed to PC2. The polyketide fusaristatin A is the metabolite contributing the most to the negative side of PC2.

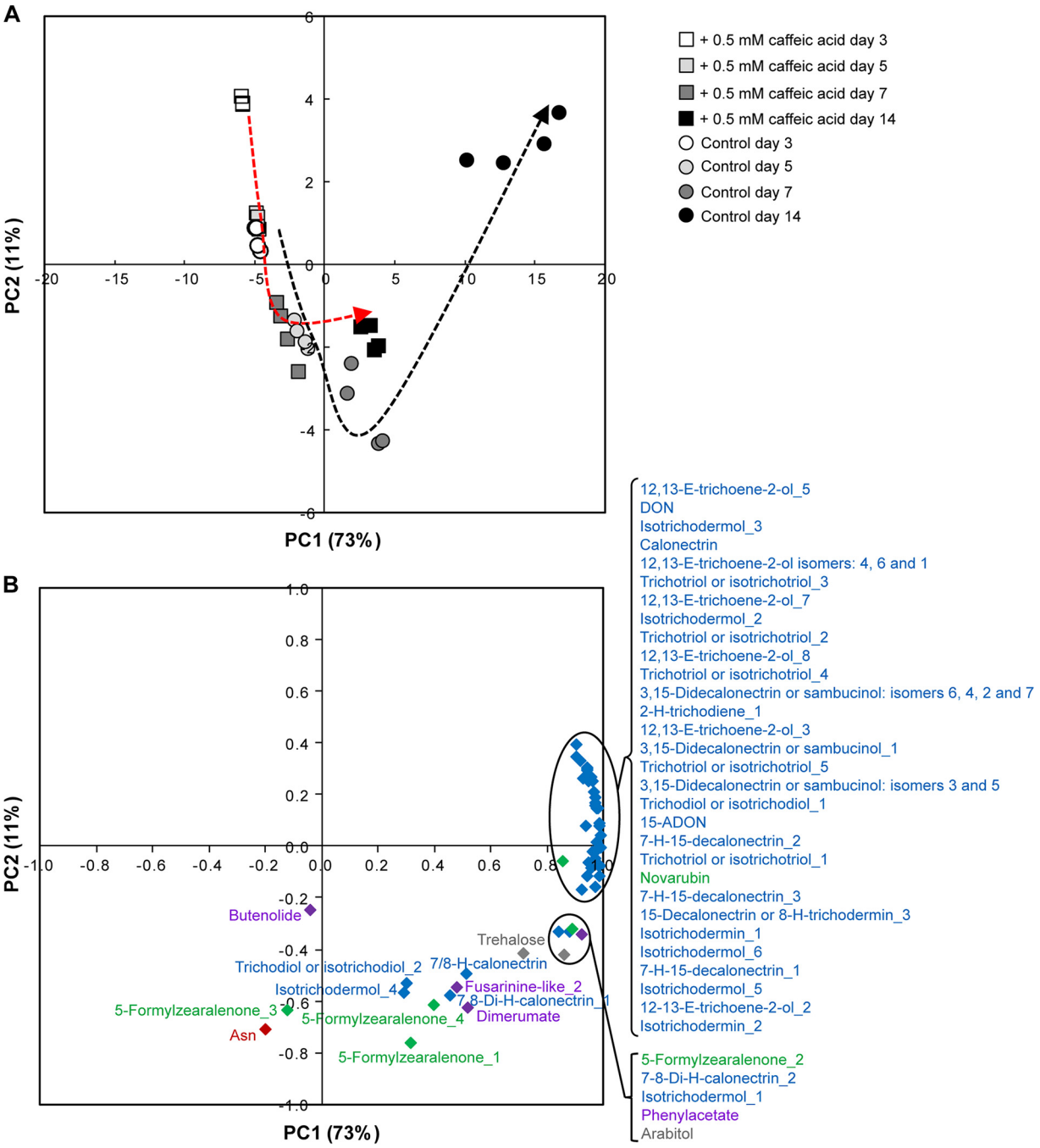

FIG 6 Caffeic acid modifies the exometabolome of *F. graminearum*. Principal-component analysis score (A) and loading (B) plots for 53 metabolites in *F. graminearum* supernatants supplemented (squares) or not (circles) with 0.5 mM caffeic acid are shown. White, day 3; light gray, day 5; dark gray, day 7; black, day 14. The names of the metabolites are reported: gray, sugars and polyols; red, amino acids and amino acid derivatives; blue, sesquiterpenes; green, polyketides; and purple, others. H, hydroxy; E, epoxy.

Concerning supernatants, PCA analyses (Fig. 6A and B) suggested that control samples at day 14 (when the difference between control and treated samples was the most pronounced) contained higher levels of a range of sesquiterpenes, while caffeic acid-treated supernatants showed relative enhanced levels of polyketides (5-formylzearalenones), sugars and polyols (trehalose and arabitol), fusarinine-like_2, dimerumate, and Asn.

For mycelial metabolite data, a two-way analysis of variance (ANOVA) indicated significant effects of culture time, culture condition, and interaction between both

factors for 96%, 62%, and 56% of the total metabolites, respectively (see Table S4 in the supplemental material for *P* values). For supernatant metabolite data, a two-way ANOVA indicated significant effects of culture time, culture condition, and their interaction for 100%, 87%, and 77% of the total metabolites, respectively (see Table S4 for *P* values).

One-way ANOVA was then used to search for any significant effect of caffeic acid at a given culture time (Fig. 7A and B). For each culture time, to highlight the metabolomic alterations between the control and caffeic acid-treated cultures, the $\log_2$ of the ratio of the mean concentrations of each metabolite in the two culture conditions was represented in a heat map (Fig. 7A for mycelia and 7B for supernatants). Red and green colors indicate $\log_2$ ratios of more than 1 and less than 1, respectively. Regarding mycelia (Fig. 7A), the main metabolites that were negatively affected by the treatment with caffeic acid were DON and butenolide at day 5, joined by Trp at day 7 (100% inhibition efficiency with caffeic acid for the three metabolites). Similarly, although with a lower magnitude, caffeic acid supplementation resulted in a reduction of TCA organic acids (fold change of between 1.7 and 2.9 for the four TCA organic acids, mainly at days 7 and 14) and most of the TCTB intermediates. The greatest decreases were observed for 3,15-didecalonectrin, sambucinol_1 and _5, DON, and 15-ADON at 7 days of culture (fold changes of 25.2, 23.7, 13.6, and 11, respectively). At day 14, the levels of the two polyketides, fusaristatin A and rubrofusarin, were almost 13 times higher in caffeic acid-treated cultures than under the control condition, as illustrated by the red color in Fig. 7A associated with these two compounds. The heat map reported in Fig. 7A also indicates a weak increase in the amounts of most of the nucleosides/nucleotides and amino acids/amino acid derivatives quantified in mycelia during the exponential phase of growth (Ala, Arg, Gln, Pro, adenosine-like, UDP-like, and uridine-like) together with a higher accumulation of aurofusarins (days 5, 7, and 14) and oosporein (a trend for all culture times). When considering alterations of the exometabolome (Fig. 7B), the strong inhibition of 15-ADON production induced by caffeic acid was accompanied by a decrease in the levels of most secondary metabolites, with some exceptions. Indeed, several compounds identified as putative polyketides, including novarubin, 5-formylzearelone_4, and fusarinine-like_2, were detected at higher levels in caffeic acid-treated cultures (fold change close to 2 for the three metabolites at days 3, 14, and 14, respectively). Surprisingly, while our data indicated that the levels of most of the TCTB intermediates were reduced, they also showed a higher accumulation of two of them, the 7,8-di-H-calonectrin_1 and 7/8-H-calonectrin. Regarding primary metabolites, the exometabolome heat map (Fig. 7B) indicated that the decrease in DON and 15-ADON (fold change = 2 at day 14 for both DON [$P = 0.0001$] and 15-ADON [$P = 0.00006$]) was accompanied by an increase in the levels of Asn (fold change = 1.5 at day 14 [$P = 0.0151$]) and trehalose (fold change = 1.3 at day 14 [$P = 0.0022$]). Taken together, the exo- and endometabolomic data suggest that while caffeic acid inhibits the TCTB biosynthetic pathway (as illustrated by the reduced levels of DON/15-ADON and many of their biosynthetic intermediates), it promotes the production of other secondary metabolites, including several polyketides and compounds classified as "others," such as dimerumate and fusarinine-like compounds. The fold changes of the latter metabolites are between 1.8 and 2.1 at the culture time when the differences between control and caffeic acid treatments are the most important, with the exceptions of fusaristatin A and rubrofusarin, for which the fold change was close to 13. In regard to primary metabolites, our data also suggest that caffeic acid affects the accumulation of the majority of detected amino acids and sugars while slightly reducing the amounts of organic acids of the TCA cycle.

DISCUSSION

Our study has implemented an original experimental approach, based on the combination of ^{1}H NMR and LC-QTOF-MS technologies, to investigate and compare the exo- and endometabolomes of *F. graminearum* cultured in DON-inducing and DON-repressing media. Most of the previously published studies that have addressed the *F.*

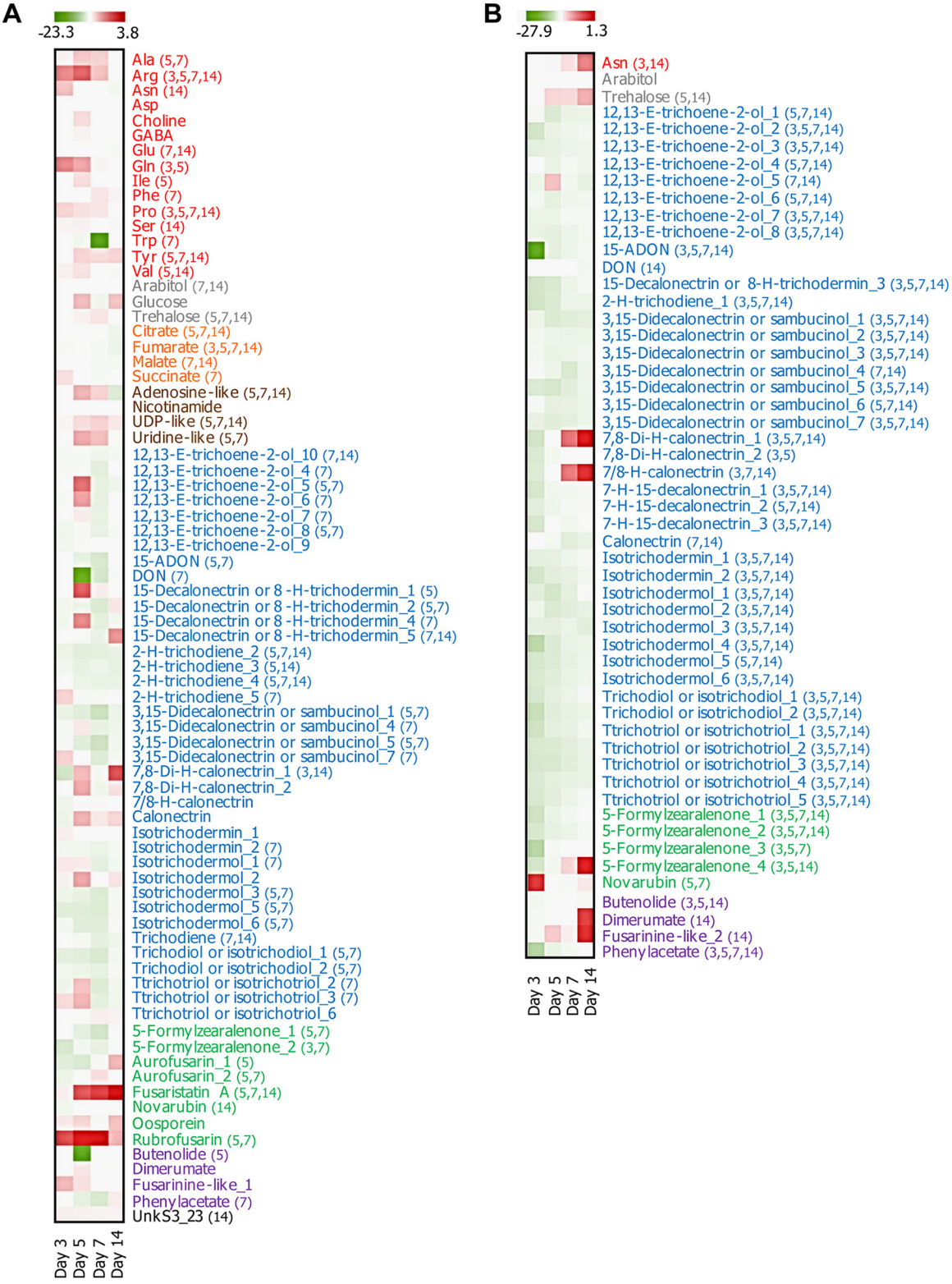

FIG 7 Integrative overview of the metabolic changes induced by caffeic acid over the time of culture. Heat maps of relative metabolite contents of *F. graminearum* in mycelia (A) and in supernatants (B) are shown. Metabolite levels were expressed as $\log_2$ ratios of values from caffeic acid-treated over control samples. The red color indicates increased metabolite levels in caffeic acid-treated samples, and the green color represents decreased metabolite levels. The numbers in parentheses indicate the times of culture for which significant differences between caffeic acid-supplemented and control treatments were statistically evident (one-way ANOVA, $P < 0.05$). H, hydroxy; E, epoxy.

graminearum metabolome (15, 20) were based on the sole use of ^{1}H NMR and were restricted to the central metabolome. Combining LC-QTOF-MS and ^{1}H NMR profiling, as in the present study, allowed maximizing the coverage of the metabolome by expanding the set of detected metabolites to semipolar ones, including secondary metabolites. Our data therefore provide an *F. graminearum* metabolome framework for future studies comparing culture conditions and predicting the production of DON.

Endo- and exometabolomes of *F. graminearum*. Ninety-five metabolites were putatively or unambiguously identified, including 26 primary metabolites and 69 secondary metabolites. As demonstrated by the PCA analyses reported in Fig. 5 and 6, most of the detected secondary metabolites were produced during the stationary phase (days 7 and 14), supporting their tight association with fungal cell differentiation or development (30). Primary metabolites were detected mainly in mycelia and included a range of amino acids and derivatives, intermediates of the TCA cycle, sugars and polyols, nucleosides, and nucleotides. Among the 69 secondary metabolites detected, a large share were putatively assigned to intermediates of the TCTB pathway. Actually, only 11 end products of secondary biosynthetic pathways have been identified, including the DON, 15-ADON, and sambucinol sesquiterpenes, the aurofusarin, rubrofusarin, and novarubin naphthoquinone pigments, the fusaristatin A lipopeptide, oosporein, formylzearalenone, butenolide, and a compound designated fusarinine-like. While 11 end products may seem quite low compared to the arsenal of 15 *PKS* and 19 *NRPS* genes present in the *F. graminearum* genome (22) and to the 67 secondary metabolite clusters predicted by Sieber et al. (31), several considerations should be borne in mind. First, among the 67 clusters predicted by Sieber et al. (31), the production of 20, which are not yet associated with a known metabolite, may be triggered exclusively by plant defense mechanisms during fungal infection. More generally, it is well established that many of the genes involved in secondary metabolic pathways are expressed only under very specific conditions (32), which might not have been met under the incubation and culture medium conditions used in the present study. Since TCTB mycotoxins were the core metabolites of this study, we used a mycotoxin synthetic culture medium which had been optimized for DON production without checking other fungal metabolites (33). Also, the goal of the extraction protocols applied in metabolomic approaches (ethanol-water and methanol-water were used in our study for ^{1}H NMR and LC-MS, respectively) is to attain a reproducible and comprehensive metabolite extraction, which may lead to a nonoptimal extraction for some secondary metabolites that may not be detectable due to masking effects of other metabolites. Nonoptimal culture conditions for the biosynthesis of fusarielin combined with nonoptimal extraction procedures are certainly the reasons why fusarielin was not detected in our glucose-based medium. Indeed production of fusarielin was shown to be significantly enhanced when cellobiose or fructose was used instead of glucose (23). Similarly, it seems that synthetic culture media do not allow the production of detectable amounts of orsellinic acid and orcinol by *F. graminearum* (34), since the authors of the previous studies were not able to detect the production of these two metabolites in a culture with a composition closely resembling that of the mycotoxin synthetic medium without the use of a mutant strain that overexpresses the corresponding *PKS14*. In regard to nonribosomal polyketides, the two iron-chelating siderophores malonichrome and ferricrocin, which have been recently shown to play critical roles in the sexual and pathogenic development of *F. graminearum* (35), were not detected in our study. The presence of iron in our culture medium is certainly the most likely explanation, since production of these siderophores has been shown to be induced by iron starvation (36). Among the secondary metabolites that were evidenced by our analysis, DON and 15-ADON, butenolide, fusaristatin A, and fusarinine-like compounds, together with the aurofusarin and rubrofusarin pigments, have been frequently reported in previously published studies that have addressed the secondary metabolism of *F. graminearum* (22, 23, 37). More rarely reported metabolites were also observed in the samples we analyzed, including sambucinol, formylzearalenone, and

oosporein. The production of the nontrichothecene sesquiterpene sambucinol was, however, not surprising, supporting the previous reports of Langseth et al. (38) and McCormick et al. (39), who illustrated the ability of *F. graminearum* to produce this metabolite. In regard to formylzearalenone, few reports have documented its biosynthesis by *F. graminearum*, with the exception of the study published by Pfeiffer et al. (40), who detected this metabolite in *F. graminearum* cultures. Our analyses have reported the potential production of a compound putatively assigned as oosporein, according to its LC-MS characteristics. Oosporein is a fungal bibenzoquinone exhibiting numerous biological and pharmacological activities. Its complete biosynthetic pathway was recently elucidated by Feng et al. (41), who demonstrated that oosporein results from the hydroxylation of orsellinic acid followed by an oxidation and a dimerization step. Therefore, the presence of oosporein in our analysis could be tightly linked with the ability of *F. graminearum* to produce orsellinic acid (22).

Caffeic acid modifies both the endo- and exometabolomes of *F. graminearum*, supporting the existence of connections between secondary and primary metabolisms. In a second step, we investigated the effect of a caffeic acid stress on endo- and exometabolome changes in *F. graminearum* cultures. In accordance with previously published data (24), 0.5 mM caffeic acid significantly decreased the production of TCTB, while no significant effect on the fungal biomass was evidenced. Caffeic acid belongs to the class of cinnamic acid derivatives, and our results demonstrate once again the high efficiency of this class of phenylpropanoids in inhibiting the biosynthesis of TCTB (42). As previously reported for other mycotoxin inhibitors (43), we also observed that addition of caffeic acid during spore germination has a lasting effect on TCTB accumulation, even though the added caffeic acid was not detectable in the culture supernatants as early as day 3. Since we previously demonstrated that the major degradation product of caffeic acid in the presence of *F. graminearum* was protocatechuic acid and that this phenolic compound has no effect on TCTB production (24), it is very unlikely that the lasting effect of caffeic acid could be attributed to a product of its metabolism. No traces of protocatechuic acid were detected in the culture supernatants or in the mycelia analyzed in the present study, because the analytical protocols that have been used were not the optimal ones to reveal the presence of this caffeic acid metabolite. In agreement with the acknowledged theory that considers mycotoxins a component of the *F. graminearum* stress response system (44), our belief is that the initiation of TCTB biosynthesis is a crucial stage determining the levels of DON and 15-ADON produced in subsequent fungal developmental stages. When comparing the effect of caffeic acid on TCTB accumulation in mycelia and supernatants at the end of cultivation (day 14), our data indicated a significant reduction of TCTB in supernatants, whereas the levels of TCTB accumulated in control and caffeic acid-treated mycelia were not significantly different. These results suggest that caffeic acid can inhibit TCTB excretion, which could be related to the demonstrated ability of some phenolic acids to downregulate the expression of the *TRI12* gene, encoding a trichothecene efflux pump (45). In addition, there is evidence for the ability of phenolic acids to affect the fungal membrane permeability barrier, probably through a perturbation of the lipid bilayers causing the leakage of ions and other chemicals, leading to a modification of the electric potential of membranes (46).

Intriguingly, while 0.5 mM caffeic acid did not alter the fungal biomass, our metabolomic data have revealed that both primary and secondary metabolisms were affected. Apart from inhibition of DON and 15-ADON biosynthesis, the main changes were (i) increases in the accumulation of several secondary metabolites, including several polyketides, (ii) alteration in the TCA cycle, (iii) modifications in the metabolism of amino acids, and (iv) modifications in the metabolism of sugars. Each point is discussed below.

First, our data clearly demonstrated that caffeic acid induced changes in most of the secondary metabolites. Along with DON and 15-ADON production, the biosynthesis of butenolide was shown to be reduced under caffeic acid-treated conditions, supporting the results of Harris et al. (47), who indicated that conditions permissive to TCTB were

also permissive to butenolide. Most of TCTB intermediates were reduced by caffeic acid, in accordance with the general lower expression of *TRI* genes induced by cinnamic acids, including ferulic and caffeic acids (42, 43).

However, the amounts of two intermediates, 7,8-di-H-calonectrin and 7/8-H-calonectrin, were shown to be higher in caffeic acid-treated cultures, as though the biosynthetic step that leads to 3,15-diacetyldeoxynivalenol from di-H-calonectrin was inhibited in the presence of caffeic acid (5). To date, the biosynthetic gene responsible for this metabolic step remains unidentified. In contrast to what was observed for TCTB and butenolide, the levels of naphthoquinone pigments and formylzearalenone in supernatants and of fusaristatin A and rubrofusarin in mycelia were increased by the addition of caffeic acid. These data are consistent with the results of Gaffoor et al. (48), who have investigated the expression patterns of 15 *PKS* genes under various conditions and showed that conditions favoring the production of DON did not favor the expression of the *PKS* genes involved in aurofusarin and rubrofusarin pigments or the PKS responsible for the first step of zearalenone biosynthesis. Moreover, since the sesquiterpene and polyketide biosynthetic pathways share a precursor, acetyl coenzyme A (acetyl-CoA), we could logically assume that when the biosynthesis of DON is inhibited, a larger amount of acetyl-CoA is available for the production of polyketides.

Regarding primary metabolites, our data have shown that compared to control mycelia, caffeic acid-treated ones had significantly smaller amounts of citrate, malate, and fumarate, suggesting an interrelation between the TCTB biosynthetic pathway and the TCA cycle. A similar observation was reported by Chen et al. (20), who have investigated the metabolomic differences between a *TRI5*-deleted *F. graminearum* strain, which has lost its ability to produce TCTB, and the wild type. The suggested interdependence between mycotoxin biosynthesis and the TCA cycle is not surprising, since the production of mycotoxins is an energy-consuming pathway and the TCA cycle plays an essential role in fungal energy metabolism. Actually, most of the ATP produced in fungal cellular respiration is linked to the production of reduced electron carriers (NADH and reduced flavin adenine dinucleotide [$FADH_2$]) through the TCA cycle. A decrease in TCTB production was, however, not related to a downregulation of GABA, which was somewhat surprising given the relationship between GABA and the TCA cycle: GABA is the central metabolite of a biochemical bypass of the TCA cycle called the GABA shunt. Links between GABA metabolism and DON production have been outlined in previously published studies (15, 49). While not contradicting the occurrence of these metabolic links, our data do not provide evidence for the positive relationship between DON and GABA. In regard to amino acid metabolism, a weak increase in the amounts of most of the amino acids/amino acid derivatives was induced by caffeic acid supplementation. Since amino acids are closely related to farnesyl-pyrophosphate (FPP), the substrate of the trichodiene synthase enzyme (TRI5), via acetyl-CoA and since caffeic acid has been previously shown to downregulate the expression of the *TRI5* gene (42), we can logically assume that caffeic acid supplementation results in more FPP and consequently more acetyl-CoA being available for the amino acid metabolism. Larger amounts of acetyl-CoA can also be related to the observed alterations in the TCA cycle, which uses acetyl-CoA to produce energy precursors. In addition, the observed increase in amino acids could be attributed to an upregulation of several genes involved in their metabolism, as demonstrated by Kim et al. (50) in *Aspergillus flavus*. Interestingly, in that study, as observed in the present study, the increase in amino acids that would indicate a positive effect on fungal growth conferred by caffeic acid was not associated with a higher fungal biomass. As outlined in the heat map shown in Fig. 7A, one amino acid, Trp, showed a contrasting pattern over time, with a significant downregulation induced by caffeic acid supplementation. As Trp is a key metabolite of the shikimate pathway (also called the chorismate pathway), its decreased accumulation suggests that in addition to inhibiting the biosynthesis of sesquiterpene metabolism (TCTB), caffeic acid could lead to alterations in the shikimate-mediated secondary metabolism. This result is consistent with the capacity of caffeic acid to downregulate the expression of some fungal genes involved

in aromatic metabolism, as evidenced in *A. flavus* by Kim et al. (50). Lastly, our data indicated higher concentrations of trehalose in caffeic acid-supplemented media. This result shows that under DON-repressing conditions, there might be an increase in the conversion of glucose-6-phosphate into storage carbohydrates. A similar observation was outlined by Nasution et al. (17), who have investigated the relationships between penicillin production and central metabolism in *Penicillium chrysogenum*. In fungi, in addition to its acknowledged role in defense mechanisms against a variety of stresses, including dehydration, heat and cold treatment, and oxidative stress (51, 52), the biosynthesis of trehalose can be required for pathogenicity (53, 54). In regard to phytopathogenic *Fusarium* spp., the role of trehalose has been investigated with the use of mutant strains (55, 56). *F. graminearum* mutant strains affected in the biosynthesis of trehalose were shown to be significantly affected in their development and virulence but also in their production of DON (56). While the exact mechanism by which the biosynthetic pathway of trehalose is linked with the biosynthesis of DON has not been elucidated yet, the findings of Song et al. (56) could explain the contrasting accumulation of the two metabolites observed in the present study.

In conclusion, the use of combined ^{1}H NMR and LC-QTOF-MS has revealed that inhibiting the production of DON with caffeic acid supplementation caused widespread and significant changes in the secondary and primary metabolisms of *F. graminearum*, although the fungal growth was not affected at the dosages we applied to the fungus. These metabolic changes involved the biosynthetic pathways of a large set of secondary metabolites, including several polyketides, alterations in the TCA cycle, and modifications in the metabolisms of amino acids and sugars. While these findings provide new information on the mechanisms that govern the inhibition of TCTB production by caffeic acid, they strongly support the interdependence between the biosynthetic pathway of DON and several additional metabolic pathways, including primary and secondary ones. These outcomes provide further evidence of the multifaceted role of DON in the life cycle of *F. graminearum*, in addition to its largely documented role in pathogenicity.

MATERIALS AND METHODS

Fungal strain and culture conditions. The *F. graminearum* CBS 185.32 strain with a DON/15-ADON chemotype (Centraal bureau voor Schimmelkulturen, The Netherlands) was used throughout this work. Under our culture conditions, the 15-ADON form was predominantly produced. A stock culture was maintained at 4°C on potato dextrose agar (PDA) (Difco, Le Ponts de Claix, France) slants. Liquid culture experiments were performed in a mycotoxin synthetic medium (43). Static sterile petri dishes (55 mm in diameter) containing 8 ml of mycotoxin synthetic medium supplemented or not with 0.5 mM caffeic acid (purchased from Sigma-Aldrich, France) were inoculated with 10^4 spores/ml produced in carboxymethyl cellulose (CMC) medium (57). Fungal liquid cultures were incubated at 25°C in the dark. At the third, fifth, seventh, and fourteenth days, the culture media were removed by centrifugation and stored at −20°C until analysis, while the mycelia were washed with 5 ml of sterile water and freeze-dried for fungal biomass quantification and LC-MS and NMR metabolite profiling. It was verified that caffeic acid supplementation does not modify the pH values of the treated broths compared to those of the control. Four repetitions were made for each condition.

Extraction and LC-MS/MS analysis of TCTB. A 4-ml sample of culture medium was extracted with 8 ml of ethyl acetate. One milliliter of the organic phase was evaporated to dryness at 70°C under a nitrogen flux.

TCTBs in mycelia were extracted by agitating 10 mg of freeze-dried and ground mycelium using 3 ml of acetonitrile-water (84:16, vol/vol) for 60 min. After centrifugation (5 min at 10,000 × *g*), 2 ml was evaporated to dryness at 70°C under a nitrogen flux.

Before LC-MS analysis, dried samples were dissolved in 400 μl of methanol-water (50:50, vol/vol) and filtered through 0.22-μm-pore-size filters. LC-tandem MS (LC-MS/MS analyses) were performed using a QTrap 2000 LC-MS/MS system (Applied Biosystems, Les Ulis, France) equipped with a TurbolonSpray electrospray ionization (ESI) source and a 1100 series high-pressure liquid chromatography (HPLC) system (Agilent, France). Chromatographic separation was achieved at 30°C with a Zorbax eclipse column (XDB C_{18}; 2.1 by 150 mm, 5-μm inner diameter; Agilent, France) and a mobile phase consisting of water-methanol (10:90, vol/vol) (solvent A) and water-methanol (90:10, vol/vol) (solvent B). Gradient elution was as follows: 8 min held at 10% solvent A, 2-min linear gradient from 10 to 70% solvent A, 2-min linear gradient from 70 to 100% solvent A, 10 min held at 100% solvent A, 1-min linear gradient from 100 to 10% solvent A, and 15 min held at 10% solvent A. The flow rate was kept at 250 μl/min The injection volume was 20 μl. The electrospray interface was used in the negative-ion mode at 400°C with the following settings: curtain gas, 20 lb/in^2; nebulizer gas, 30 lb/in^2; auxiliary gas, 70 lb/in^2; ion spray voltage, −4,200 V; declustering potential, −30 V; entrance potential, −10 V; collision energy, −30 eV;

collision-activated dissociation gas, medium. Highly concentrated samples were diluted when necessary. The MRM mode was used for quantification. Transitions used were 295→265 for DON and 337→150 for 15-ADON. Quantification was performed using external calibration with DON and 15-ADON standard solutions (Romer Labs, Austria), ranging from 10 to 1,000 ng/ml.

LC-QTOF-MS analysis of semipolar metabolites. LC-QTOF-MS analyses were performed on culture supernatants and methanolic extracts of freeze-dried and ground mycelia. For each mycelium sample, 20 mg of powder was suspended with 1 ml of methanol-water (70:30, vol/vol) acidified with formic acid (0.1%) and containing 1.37 mM methyl vanillate (Sigma-Aldrich, France) as an internal standard. The suspension was sonicated for 15 min in an ice bath, centrifuged, and filtered on a 0.22-μm polyvinylidene difluoride (PVDF) filter (Millex Millipore, Billerica, MA, USA) in HPLC vials. Filtered samples were stored at −20°C until analysis. Culture supernatants were filtered on a 0.22-μm PVDF filter (Millex Millipore, Billerica, MA, USA) in HPLC vials.

An Ultimate 3000 HPLC (Dionex, Sunnyvale, CA, USA) was used to separate metabolites on a reversed-phase C_{18} column (150 by 2.0 mm, 3-μm inner diameter; Phenomenex, Le Pecq, France) using 0.1% formic acid in water as solvent A, acetonitrile as solvent B, and the following gradient: 0 to 5 min, 3% B; 5 to 35 min, 3% to 95%, linear; 35 to 40 min, 95%; 40 to 41 min, 95% to 3%, linear; and 41 to 56 min, 3%. The flow rate was set at 350 μl/min. The column temperature was set at 30°C. The injection volume was 5 μl. Metabolites were detected using a quadrupole time of flight (QTOF) mass spectrometer (Bruker, Bremen, Germany). Electrospray ionization in positive mode was used. The scan rate for ions at an *m/z* range of 50 to 1200 was fixed at 2 spectra per second. Other parameters were as follows: capillary voltage, 4,500 V; end plate voltage, 500 V; nebulizer pressure (N_2), 2.4 × 10^5 Pa; dry gas (N_2), 8.0 liters/min; and dry heater, 190°C. The *m/z* scale was calibrated with a 10 mM formiate lithium solution. Each extracted sample was injected twice as technological replicates. One sample was used as a quality control (QC) sample and injected each 10 injections. A blank extraction was also injected to identify potential contaminants. Raw data were processed in a targeted manner using the QuantAnalysis 2.0 software (Bruker, Bremen, Germany). A list of candidate compounds was established according to literature data on fungal metabolites, and the corresponding *m/z* ratios were looked for in all sample analyses.

^{1}H NMR analysis of polar metabolites. ^{1}H NMR analyses were performed on polar extracts of freeze-dried mycelium powder samples and filtered mycelium culture supernatants. For mycelium, polar metabolites were extracted with an ethanol-water series adapted from that described by Moing et al. (58). Briefly, for each sample, 30 mg of lyophilized mycelium powder was successively extracted with 2 ml 80% (vol/vol) ethanol-water, 2 ml 50% (vol/vol) ethanol-water, and 3 ml water at 80°C for 15 min. The three supernatants were pooled, dried under vacuum, and lyophilized. The pHs of dried extracts were adjusted with deuterated potassium hydroxide (KOD) to an apparent value of 6.00 in 100 mM potassium phosphate deuterated buffer solution containing 2 mM EDTA, using the BTpH Bruker titration robot (Bruker Biospin, Rheinstetten, Germany), and lyophilized again. The pH-adjusted extracts were stored in the dark under vacuum at room temperature before ^{1}H NMR analysis was completed within 1 week. ^{1}H NMR spectra were recorded on each pH-adjusted extract solubilized in 0.5 ml D_2O (Eurisotop, Saint-Aubin, France) added with sodium salt of (trimethylsilyl)propionic-2,2,3,3-D_4 acid (TSP) at a final concentration of 0.01% (mg/ml) for chemical shift calibration. The mixture was centrifuged at 17,700 × *g* for 5 min at room temperature, and the supernatant was then transferred into a 5-mm NMR tube (507-PP7; Wilmad, Vineland, NJ, USA) for acquisition.

Culture supernatants were filtered at 0.22 μm (Millex Millipore, Billerica, MA, USA). Five hundred microliters of filtrate was added with 50 μl of D_2O and with 5 μl of TSP solution (final concentration, 0.01 mg/ml) for chemical shift calibration and transferred into a 5-mm NMR tube (507-PP7; Wilmad, Vineland, NJ, USA) for acquisition.

NMR spectra were acquired at 500.162 MHz at 300 K on an Avance III spectrometer (Bruker Biospin, Wissembourg, France) using a 5-mm ATMA broadband inverse probe flushed with nitrogen gas. For mycelium extracts, 64 scans of 32,000 data points were acquired with a single-pulse sequence (zg), a 90° pulse angle, a spectral width of 6,000 Hz, an acquisition time of 2.73 s, and a recycle delay of 20 s. For culture supernatants, 128 scans of 64,000 data points were acquired with a water suppression pulse sequence (noesygpppr1d), a 90° pulse angle, a spectral width of 10,000 Hz, an acquisition time of 3.28 s, a mixing time of 10 ms, and a recycle delay of 2 s. An automation procedure (automatic sample loading, 90-s temperature equilibration time, automatic tuning and matching, and automatic shimming with Topshim) was used for data acquisition. Preliminary data processing was carried out with TopSpin 3.0 software (Bruker Biospin, Karlsruhe, Germany). Each free induction decay (FID) was Fourier transformed (0.3-Hz line broadening), manually phased, and baseline corrected. The resulting spectra were calibrated by setting the TSP signal to 0 ppm.

The assignments of metabolites in the NMR spectra were made by comparing the proton chemical shifts with literature (59) and database (MeRy-B 2011, HMDB, and BMRB) values, by comparison with spectra of authentic compounds recorded under the same buffer solution conditions, and by spiking the samples. Two-dimensional (2D) homonuclear correlation spectroscopy (COSY) experiments were carried out to verify the identities of known compounds.

Absolute metabolite concentrations of mycelium extracts in the NMR tube were calculated using the Analytical Profiler mode of AMIX software (version 3.9.10; Bruker Biospin, Karlsruhe, Germany) for calculation of resonance areas, followed by data export to Excel software (Microsoft, Redmond, WA, USA). For absolute quantification with an electronic reference (Digital ERETIC; Bruker TopSpin 3.0), 4 calibration curves (glucose and fructose, 2.5 to 100 mM; glutamate and glutamine, 0 to 30 mM) were prepared and analyzed under the same conditions. The glucose calibration was used for the quantification of all

compounds as a function of the number of protons of selected resonances, except for fructose, glutamate, and glutamine, which were quantified using their own calibration curve. Then the metabolite content in each sample was calculated from concentrations in the NMR tube and sample dry weight. The content of each organic or amino acid was expressed as grams of the acid form per weight unit. The content of NMR unknown compounds (named using the middle value of the chemical shift and the multiplicity of the corresponding resonance group, e.g., unknS3.23 for a singlet at 3.23 ppm) was calculated hypothesizing that the observed resonance corresponded to one proton and using an arbitrary molecular mass of 100 Da. The concentrations of metabolites identified in the culture supernatants were determined after integration of selected resonances of interest in the ^{1}H NMR spectra with TopSpin 3.0 and expressed in arbitrary units.

Expression of results and statistical analyses. DON and 15-ADON were quantified by LC-MS/MS, LC-QTOF-MS, and ^{1}H NMR. As results obtained by the three techniques were similar and to avoid weighing down figures, only results from LC-MS/MS were used for the statistical analyses. Data for TCTB production and fungal growth were reported as mean values ± standard deviations from four biological replications. Mean values were compared at the 5% significance level using a standard Student *t* test (control versus treated). Most of the compositional data were nonnormally distributed, as determined using the Shapiro-Wilk normality test with XLSTAT 2016 software (Addinsoft, Rennes, France). Nonnormally distributed data were log transformed as $\log_{10}$ (variable + 1) to ensure normal distributions of residues and homogeneity of variance. For all compositional data, the effects of culture time (days 3, 5, 7, and 14), condition (control/caffeic acid treatment), and their interaction were analyzed with two–way analyses of variance (ANOVAs) using R scripts in the BioStatFlow web application (biostatflow.org) ($P < 0.05$, false-discovery rate [FDR] correction). One-way ANOVA was then used to search for significant effects of culture condition at a given culture time (BioStatFlow) ($P < 0.05$, FDR correction).

Principal-component analysis (PCA) was performed using XLSTAT 2016 software after unit variance scaling of R scripts.

K-means clustering (MultiExperiment Viewer version 4.8) was performed on the means of the biological replicates (data mean centered and reduced to unit variance, Pearson correlation distance, and average linkage).

SUPPLEMENTAL MATERIAL

Supplemental material for this article may be found at https://doi.org/10.1128/AEM.01705-17.

SUPPLEMENTAL FILE 1, PDF file, 0.7 MB.

ACKNOWLEDGMENTS

We thank Sylvain Chéreau for fruitful discussions and Gisèle Marchegay for technical assistance.

F.R.-F. and A.M. conceived and designed the experiments. L.L., S.B., C.D., M.M., M.-N.V.-B., V.A.-P., and L.P.-G. performed the experiments. A.M., V.A.-P., S.B., C.D., M.M., and N.P. analyzed the data. F.R.-F., V.A.-P., A.M., S.B., and C.D. wrote the paper.

REFERENCES

1. Dean R, Van Kan JAL, Pretorius ZA, Hammond-Kosack KE, Di Pietro A, Spanu PD, Rudd JJ, Dickman M, Kahmann R, Ellis J, Foster GD. 2012. The top 10 fungal pathogens in molecular plant pathology. Mol Plant Pathol 13:414–430. https://doi.org/10.1111/j.1364-3703.2011.00783.x.
2. Yli-Mattila T. 2010. Ecology and evolution of toxigenic *Fusarium* species in cereals in northern Europe and Asia. J Plant Pathol 92:7–18.
3. Desjardins AE. 2007. *Fusarium* mycotoxins: chemistry, genetics and biology. Plant Pathol 56:2. https://doi.org/10.1111/j.1365-3059.2006.01505.x.
4. Merhej J, Richard-Forget F, Barreau C. 2011. Regulation of trichothecene biosynthesis in *Fusarium*: recent advances and new insights. Appl Microbiol Biotechnol 91:519–528. https://doi.org/10.1007/s00253-011-3397-x.
5. Kimura M, Tokai T, Takahashi-Ando N, Ohsato S, Fujimura M. 2007. Molecular and genetic studies of *Fusarium* trichothecene biosynthesis: pathways, genes, and evolution. Biosci Biotechnol Biochem 71:2105–2123. https://doi.org/10.1271/bbb.70183.
6. Alexander NJ, Proctor RH, McCormick SP. 2009. Genes, gene clusters, and biosynthesis of trichothecenes and fumonisins in *Fusarium*. Toxin Rev 28:198–215. https://doi.org/10.1080/15569540903092142.
7. Kazan K, Gardiner DM, Manners JM. 2012. On the trail of a cereal killer: recent advances in *Fusarium graminearum* pathogenomics and host resistance. Mol Plant Pathol 13:399–413. https://doi.org/10.1111/j.1364-3703.2011.00762.x.
8. Woloshuk CP, Shim WB. 2013. Aflatoxins, fumonisins, and trichothecenes: a convergence of knowledge. FEMS Microbiol Rev 37:94–109. https://doi.org/10.1111/1574-6976.12009.
9. Gardiner D, Osborne S, Kazan K, Manners J. 2009. Low pH regulates the production of deoxynivalenol by *Fusarium graminearum*. Microbiology 155:3149–3156. https://doi.org/10.1099/mic.0.029546-0.
10. Merhej J, Boutigny A, Pinson-Gadais L, Richard-Forget F, Barreau C. 2010. Acidic pH as a determinant of TRI gene expression and trichothecene B biosynthesis in *Fusarium graminearum*. Food Addit Contam A Chem 27:710–717. https://doi.org/10.1080/19440040903514531.
11. Merhej J, Richard-Forget F, Barreau C. 2011. The pH regulatory factor Pad1 regulates Tri gene expression and trichothecene production in *Fusarium graminearum*. Fungal Genet Biol 48:275–284. https://doi.org/10.1016/j.fgb.2010.11.008.
12. Montibus M, Ducos C, Bonnin-Verdal MN, Bormann J, Ponts N, Richard-Forget F, Barreau C. 2013. The bZIP transcription factor Fgap1 mediates oxidative stress response and trichothecene biosynthesis but not virulence in *Fusarium graminearum*. PLoS One 8:e83377. https://doi.org/10.1371/journal.pone.0083377.
13. Johnson CH, Gonzalez FJ. 2012. Challenges and opportunities of metabolomics. J Cell Physiol 227:2975–2981. https://doi.org/10.1002/jcp.24002.
14. Panagiotou G, Christakopoulos P, Olsson L. 2005. The influence of different cultivation conditions on the metabolome of *Fusarium oxysporum*. J Biotechnol 118:304–315. https://doi.org/10.1016/j.jbiotec.2005.05.004.

15. Lowe RGT, Allwood JW, Galster AM, Urban M, Daudi A, Canning G, Ward JL, Beale MH, Hammond-Kosack KE. 2010. Combined ^{1}H nuclear magnetic resonance and electrospray ionization–mass spectrometry analysis to understand the basal metabolism of plant-pathogenic *Fusarium spp*. Mol Plant Microbe Interact 23:1605–1618. https://doi.org/10.1094/MPMI-04-10-0092.
16. Choi JN, Kim J, Jung WH, Lee CH. 2012. Influence of iron regulation on the metabolome of *Cryptococcus neoformans*. PLoS One 7:e41654. https://doi.org/10.1371/journal.pone.0041654.
17. Nasution U, van Gulik WM, Ras C, Proell A, Heijnen JJ. 2008. A metabolome study of the steady-state relation between central metabolism, amino acid biosynthesis and penicillin production in *Penicillium chrysogenum*. Metab Eng 10:10–23. https://doi.org/10.1016/j.ymben.2007.07.001.
18. Smith JE, Lay JO, Bluhm BH. 2012. Metabolic fingerprinting reveals a new genetic linkage between ambient pH and metabolites associated with desiccation tolerance in *Fusarium verticillioides*. Metabolomics 8:376–385. https://doi.org/10.1007/s11306-011-0322-3.
19. Park SJ, Hyun SH, Suh HW, Lee SY, Sung GH, Kim SH, Choi HK. 2013. Biochemical characterization of cultivated *Cordyceps bassiana* mycelia and fruiting bodies by ^{1}H nuclear magnetic resonance spectroscopy. Metabolomics 9:236–246. https://doi.org/10.1007/s11306-012-0442-4.
20. Chen FF, Zhang JT, Song XS, Yang J, Li HP, Tang HR, Liao YC. 2011. Combined metabonomic and quantitative real-time PCR analyses reveal systems metabolic changes of *Fusarium graminearum* induced by Tri5 gene deletion. J Proteome Res 10:2273–2285. https://doi.org/10.1021/pr101095t.
21. Hansen FT, Sorensen JL, Giese H, Sondergaard TE, Frandsen RJN. 2012. Quick guide to polyketide synthase and nonribosomal synthetase genes in *Fusarium*. Int J Food Microbiol 155:128–136. https://doi.org/10.1016/j.ijfoodmicro.2012.01.018.
22. Hansen FT, Gardiner DM, Lysøe E, Fuertes PR, Tudzynski B, Wiemann P, Sondergaard TE, Giese H, Brodersen DE, Sørensen JL. 2015. An update to polyketide synthase and non-ribosomal synthetase genes and nomenclature in *Fusarium*. Fungal Genet Biol 75:20–29. https://doi.org/10.1016/j.fgb.2014.12.004.
23. Sorensen JL, Akk E, Thrane U, Giese H, Sondergaard TE. 2013. Production of fusarielins by *Fusarium*. Int J Food Microbiol 160:206–211. https://doi.org/10.1016/j.ijfoodmicro.2012.10.016.
24. Gauthier L, Bonnin-Verdal M-N, Marchegay G, Pinson-Gadais L, Ducos C, Richard-Forget F, Atanasova-Penichon V. 2016. Fungal biotransformation of chlorogenic and caffeic acids by *Fusarium graminearum*: new insights in the contribution of phenolic acids to resistance to deoxynivalenol accumulation in cereals. Int J Food Microbiol 221:61–68. https://doi.org/10.1016/j.ijfoodmicro.2016.01.005.
25. Geng ZY, Zhu W, Su H, Zhao Y, Zhang KQ, Yang JK. 2014. Recent advances in genes involved in secondary metabolite synthesis, hyphal development, energy metabolism and pathogenicity in *Fusarium graminearum* (teleomorph *Gibberella zeae*). Biotechnol Adv 32:390–402. https://doi.org/10.1016/j.biotechadv.2013.12.007.
26. Keller NP, Turner G, Bennett JW. 2005. Fungal secondary metabolism—from biochemistry to genomics. Nat Rev Microbiol 3:937–947. https://doi.org/10.1038/nrmicro1286.
27. Nielsen KF, Mogensen JM, Johansen M, Larsen TO, Frisvad JC. 2009. Review of secondary metabolites and mycotoxins from the *Aspergillus niger* group. Anal Bioanal Chem 395:1225–1242. https://doi.org/10.1007/s00216-009-3081-5.
28. Sumner LW, Amberg A, Barrett D, Beale MH, Beger R, Daykin CA, Fan TWM, Fiehn O, Goodacre R, Griffin JL, Hankemeier T, Hardy N, Harnly J, Higashi R, Kopka J, Lane AN, Lindon JC, Marriott P, Nicholls AW, Reily MD, Thaden JJ, Viant MR. 2007. Proposed minimum reporting standards for chemical analysis: Chemical Analysis Working Group (CAWG) Metabolomics Standards Initiative (MSI). Metabolomics 3:211–221. https://doi.org/10.1007/s11306-007-0082-2.
29. Sørensen JL, Sondergaard TE, Covarelli L, Fuertes PR, Hansen FT, Frandsen RJN, Saei W, Lukassen MB, Wimmer R, Nielsen KF, Gardiner DM, Giese H. 2014. Identification of the biosynthetic gene clusters for the lipopeptides fusaristatin A and W493 B in *Fusarium graminearum* and *F. pseudograminearum*. J Nat Prod 77:2619–2625. https://doi.org/10.1021/np500436r.
30. Calvo AM, Wilson RA, Bok JW, Keller NP. 2002. Relationship between secondary metabolism and fungal development. Microbiol Mol Biol Rev 66:447–459. https://doi.org/10.1128/MMBR.66.3.447-459.2002.
31. Sieber CMK, Lee W, Wong P, Münsterkötter M, Mewes H-W, Schmeitzl C, Varga E, Berthiller F, Adam G, Güldener U. 2014. The *Fusarium graminearum* genome reveals more secondary metabolite gene clusters and hints of horizontal gene transfer. PLoS One 9:e110311. https://doi.org/10.1371/journal.pone.0110311.
32. Brakhage AA. 2013. Regulation of fungal secondary metabolism. Nat Rev Microbiol 11:21–32. https://doi.org/10.1038/nrmicro2916.
33. Boutigny A-L. 2007. Etude de l'effet de composés du grain de blé dur sur la régulation de la voie de biosynthèse des trichothécènes B purification de composés inhibiteurs, analyse des mécanismes impliqués. Doctoral thesis. Université de Bordeaux, Bordeaux, France. http://grenet.drimm.u-bordeaux1.fr/pdf/2007/BOUTIGNY_ANNE-LAURE_2007.pdf
34. Jørgensen SH, Frandsen RJN, Nielsen KF, Lysøe E, Sondergaard TE, Wimmer R, Giese H, Sørensen JL. 2014. *Fusarium graminearum* PKS14 is involved in orsellinic acid and orcinol synthesis. Fungal Genet Biol 70:24–31. https://doi.org/10.1016/j.fgb.2014.06.008.
35. Oide S, Berthiller F, Wiesenberger G, Adam G, Turgeon BG. 2014. Individual and combined roles of malonichrome, ferricrocin, and TAFC siderophores in *Fusarium graminearum* pathogenic and sexual development. Front Microbiol 5:759. https://doi.org/10.3389/fmicb.2014.00759.
36. Haas H. 2014. Fungal siderophore metabolism with a focus on *Aspergillus fumigatus*. Nat Prod Rep 31:1266–1276. https://doi.org/10.1039/C4NP00071D.
37. Hegge A, Lønborg R, Nielsen D, Sørensen J. 2015. Factors influencing production of fusaristatin A in *Fusarium graminearum*. Metabolites 5:184–191. https://doi.org/10.3390/metabo5020184.
38. Langseth W, Ghebremeskel M, Kosiak B, Kolsaker P, Miller D. 2001. Production of culmorin compounds and other secondary metabolites by *Fusarium culmorum* and *F. graminearum* strains isolated from Norwegian cereals. Mycopathologia 152:23–34. https://doi.org/10.1023/A:1011964306510.
39. McCormick SP, Alexander NJ, Harris LJ. 2010. CLM1 of *Fusarium graminearum* encodes a longiborneol synthase required for culmorin production. Appl Environ Microbiol 76:136–141. https://doi.org/10.1128/AEM.02017-09.
40. Pfeiffer E, Hildebrand AA, Becker C, Schnattinger C, Baumann S, Rapp A, Goesmann H, Syldatk C, Metzler M. 2010. Identification of an aliphatic epoxide and the corresponding dihydrodiol as novel congeners of zearalenone in cultures of *Fusarium graminearum*. J Agric Food Chem 58:12055–12062. https://doi.org/10.1021/jf1022498.
41. Feng P, Shang Y, Cen K, Wang C. 2015. Fungal biosynthesis of the bibenzoquinone oosporein to evade insect immunity. Proc Natl Acad Sci U S A 112:11365–11370. https://doi.org/10.1073/pnas.1503200112.
42. Atanasova-Penichon V, Barreau C, Richard-Forget F. 2016. Antioxidant secondary metabolites in cereals: potential involvement in resistance to *Fusarium* and mycotoxin accumulation. Front Microbiol 7:566. https://doi.org/10.3389/fmicb.2016.00566.
43. Boutigny A-L, Barreau C, Atanasova-Penichon V, Verdal-Bonnin M-N, Pinson-Gadais L, Richard-Forget F. 2009. Ferulic acid, an efficient inhibitor of type B trichothecene biosynthesis and Tri gene expression in *Fusarium* liquid cultures. Mycol Res 113:746–753. https://doi.org/10.1016/j.mycres.2009.02.010.
44. Ponts N. 2015. Mycotoxins are a component of *Fusarium graminearum* stress-response system. Front Microbiol 6:1234. https://doi.org/10.3389/fmicb.2015.01234.
45. Ferruz E, Atanasova-Pénichon V, Bonnin-Verdal MN, Marchegay G, Pinson-Gadais L, Ducos C, Lorán S, Ariño A, Barreau C, Richard-Forget F. 2016. Effects of phenolic acids on the growth and production of T-2 and HT-2 toxins by *Fusarium langsethiae* and *F. sporotrichioides*. Molecules 21:449. https://doi.org/10.3390/molecules21040449.
46. Sung WS, Lee DG. 2010. Antifungal action of chlorogenic acid against pathogenic fungi, mediated by membrane disruption. Pure Appl Chem 82:219–226. https://doi.org/10.1351/PAC-CON-09-01-08.
47. Harris LJ, Alexander NJ, Saparno A, Blackwell B, McCormick SP, Desjardins AE, Robert LS, Tinker N, Hattori J, Piché C, Schernthaner JP, Watson R, Ouellet T. 2007. A novel gene cluster in *Fusarium graminearum* contains a gene that contributes to butenolide synthesis. Fungal Genet Biol 44:293–306. https://doi.org/10.1016/j.fgb.2006.11.001.
48. Gaffoor I, Brown DW, Plattner R, Proctor RH, Qi W, Trail F. 2005. Functional analysis of the polyketide synthase genes in the filamentous fungus *Gibberella zeae* (anamorph *Fusarium graminearum*). Eukaryot Cell 4:1926–1933. https://doi.org/10.1128/EC.4.11.1926-1933.2005.
49. Bönnighausen J, Gebhard D, Kröger C, Hadeler B, Tumforde T, Lieberei R, Bergemann J, Schäfer W, Bormann J. 2015. Disruption of the GABA shunt affects mitochondrial respiration and virulence in the cereal pathogen

Fusarium graminearum. Mol Microbiol 98:1115–1132. https://doi.org/10.1111/mmi.13203.
50. Kim JH, Yu J, Mahoney N, Chan KL, Molyneux RJ, Varga J, Bhatnagar D, Cleveland TE, Nierman WC, Campbell BC. 2008. Elucidation of the functional genomics of antioxidant-based inhibition of aflatoxin biosynthesis. Int J Food Microbiol 122:49–60. https://doi.org/10.1016/j.ijfoodmicro.2007.11.058.
51. Cao Y-R, Chen S-Y, Zhang J-S. 2008. Ethylene signaling regulates salt stress response: an overview. Plant Signal Behav 3:761–763. https://doi.org/10.4161/psb.3.10.5934.
52. Elbein AD, Pan YT, Pastuszak I, Carroll D. 2003. New insights on trehalose: a multifunctional molecule. Glycobiology 13:17–27. https://doi.org/10.1093/glycob/cwg047.
53. Cervantes-Chávez JA, Valdés-Santiago L, Bakkeren G, Hurtado-Santiago E, León-Ramírez CG, Esquivel-Naranjo EU, Landeros-Jaime F, Rodríguez-Aza Y, Ruiz-Herrera J. 2016. Trehalose is required for stress resistance and virulence of the Basidiomycota plant pathogen *Ustilago maydis*. Microbiology 162:1009–1022. https://doi.org/10.1099/mic.0.000287.
54. Tournu H, Fiori A, Van Dijck P. 2013. Relevance of trehalose in pathogenicity: some general rules, yet many exceptions. PLoS Pathog 9:e1003447. https://doi.org/10.1371/journal.ppat.1003447.
55. Boudreau BA, Larson TM, Brown DW, Busman M, Roberts ES, Kendra DF, McQuade KL. 2013. Impact of temperature stress and validamycin A on compatible solutes and fumonisin production in *F. verticillioides*: role of trehalose-6-phosphate synthase. Fungal Genet Biol 57:1–10. https://doi.org/10.1016/j.fgb.2013.06.001.
56. Song X-S, Li H-P, Zhang J-B, Song B, Huang T, Du X-M, Gong A-D, Liu Y-K, Feng Y-N, Agboola RS, Liao Y-C. 2014. Trehalose 6-phosphate phosphatase is required for development, virulence and mycotoxin biosynthesis apart from trehalose biosynthesis in *Fusarium graminearum*. Fungal Genet Biol 63:24–41. https://doi.org/10.1016/j.fgb.2013.11.005.
57. Montibus M, Khosravi C, Zehraoui E, Verdal-Bonnin M-N, Richard-Forget F, Barreau C. 2016. Is the Fgap1 mediated response to oxidative stress chemotype dependent in *Fusarium graminearum*? FEMS Microbiol Lett 363:1–7. https://doi.org/10.1093/femsle/fnv232.
58. Moing A, Maucourt M, Renaud C, Gaudillè M, Brouquisse R, Lebouteiller B, Gousset-Dupont A, Vidal J, Granot D, Denoyes-Rothan B, Lerceteau-Köhler E, Rolin D. 2004. Quantitative metabolic profiling by 1-dimensional ^{1}H-NMR analyses: application to plant genetics and functional genomics. Funct Plant Biol 31:889–902. https://doi.org/10.1071/FP04066.
59. Fan TWM. 1996. Metabolite profiling by one- and two-dimensional NMR analysis of complex mixtures. Prog Nucl Magn Reson Spectrosc 28:161–219.